Electronic Supplementary Material (ESI) for Journal of Materials Chemistry C.

Supporting Information

Tuning Optoelectronic Characteristics of Ionic Organic Crystalline Assemblies

Bryan Borders,[a] Morteza Adinehnia,[a] Bhaskar Chilukuri,[a] Michael Ruf,[b] K. W. Hipps,[a] * Ursula Mazur[a] *

[a] Department of Chemistry and Materials Science and Engineering Program, Washington State University, Pullman, WA, 99164-4630, USA

[b] Bruker AXS Inc., Madison, WI, 53711, USA

X-ray photoelectron spectroscopy (XPS) Measurements

Experimental

The X-ray photoelectron spectroscopy (XPS) analysis was performed using Kratos Analytical Axis 165 ESCA spectrometer equipped with an Al Kα source (energy:1486.6 eV., Linewidth:0.85). The binding energy was referenced to C1s signal at 285 eV. Charging in the sample was neutralized by an electron flood gun (Filament current: 1.78 A, Filament bias: 1.2 V and Charge balance: 2.7 V). CasaXPS (Casa Software Ltd.) was used to quantify the collected spectra. All samples were prepared by embedding a crystalline powder specimen into a thin high purity indium foil pressed on the XPS stub.

Results

The XPS data for H_2TMPyP:H_2TSPP was reported earlier.[1] A high resolution scan of the N 1s region of the H_2TMPyP:NiTSPP and the H_2TMPyP:CuTSPP crystals are shown in figures S1 and S2, respectively. The H_2TMPyP tectons present in both crystal systems have three types of nitrogens. The porphyrin ring has imine (–C=N–) nitrogens with binding energy near 398 eV and the pyrrole (–NH–) nitrogens at 400 eV.[2,3] The four equivalent nitrogens of the *meso* N-methyl-pyridinium substituents appear near 402 eV.[4,5] Both the NiTSPP and the CuTSPP have four equivalent nitrogens each with binding energy near 398.5 eV[6]. The ratio of the areas under the three nitrogen peaks in figures S1 and S3 are 6:4:2 (right to left peaks). In Figure S3 the nickel Ni $2p_{1/2}$ signal in the H_2TMPyP:NiTSPP crystals is at 870 eV. Two small features that appear at 862 eV and 876 eV are satellites peaks, respectively, from Ni $2p_{3/2}$ and Ni $2p_{1/2}$. In Figure S4 the Cu $2p_{3/2}$ signal is at 933 eV and Cu $2p_{1/2}$ peak appears at 953 eV. A strong Cu $2p_{3/2}$ satellite peak is observed at 942 eV.[7] A Cu$2p_{1/2}$ satellite peak which typically appears at 962 eV is not shown in the figure.

The XPS quantification measurements corroborate a 1:1 ionic tecton composition for both the H_2TMPyP:NiTSPP and the H_2TMPyP:CuTSPP crystals. See Table S1 for details.

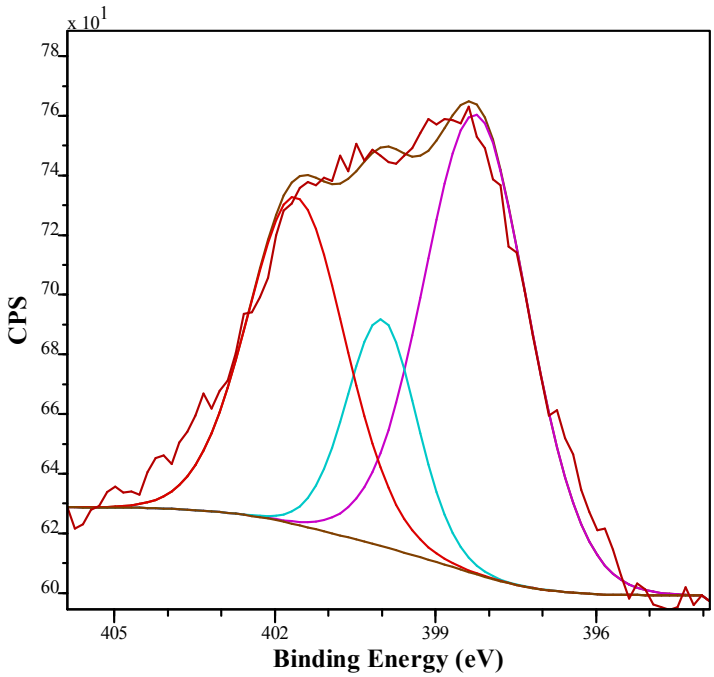

Fig. S1 High resolution XPS spectrum of N 1s peaks of H_2TMPyP:NiTSPP, showing a 6:4:2 ratio of Ni-N and imine: pyrrole: N-methyl-pyridinium nitrogens.

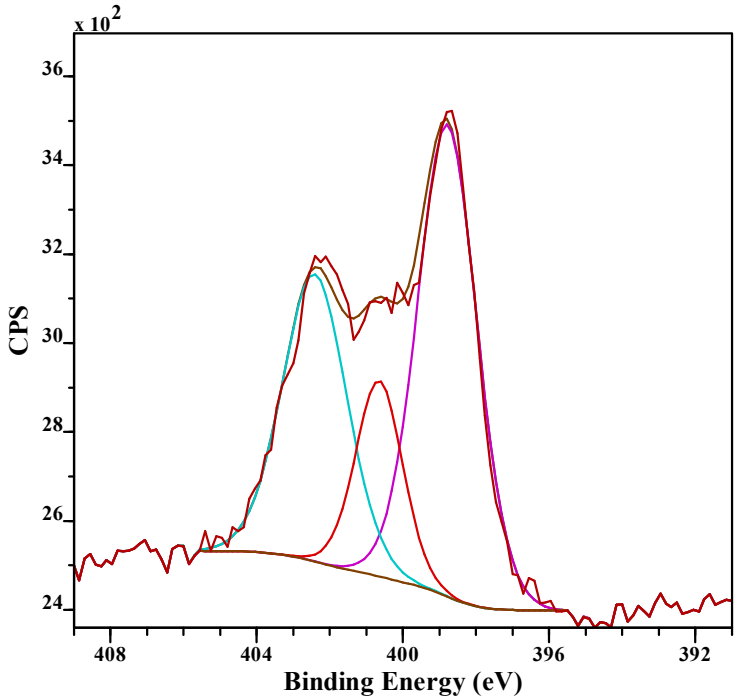

Fig. S2 High resolution XPS spectrum of N 1s peaks of H_2TMPyP:CuTSPP, showing a 6:4:2 ratio of Cu-N and imine: pyrrole: N-methyl-pyridinium nitrogens.

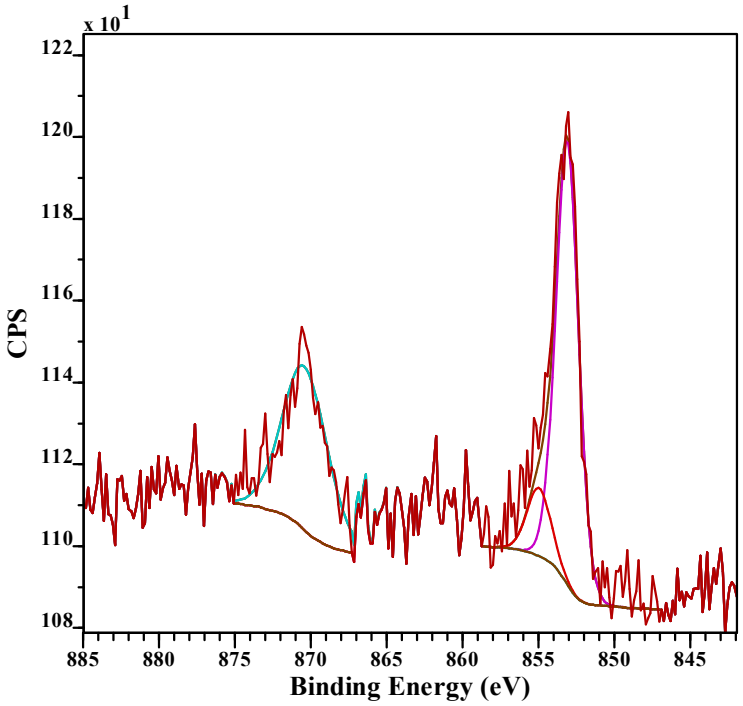

Fig. S3 High resolution XPS spectrum of Ni 2p of H_2TMPyP:NiTSPP.

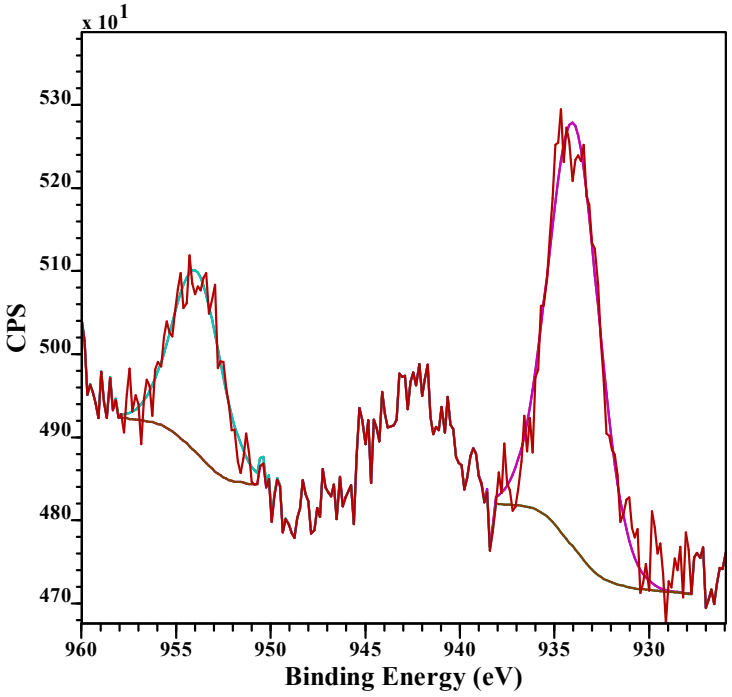

Fig. S4 High resolution XPS spectrum of Cu 2p in H_2TMPyP:CuTSPP.

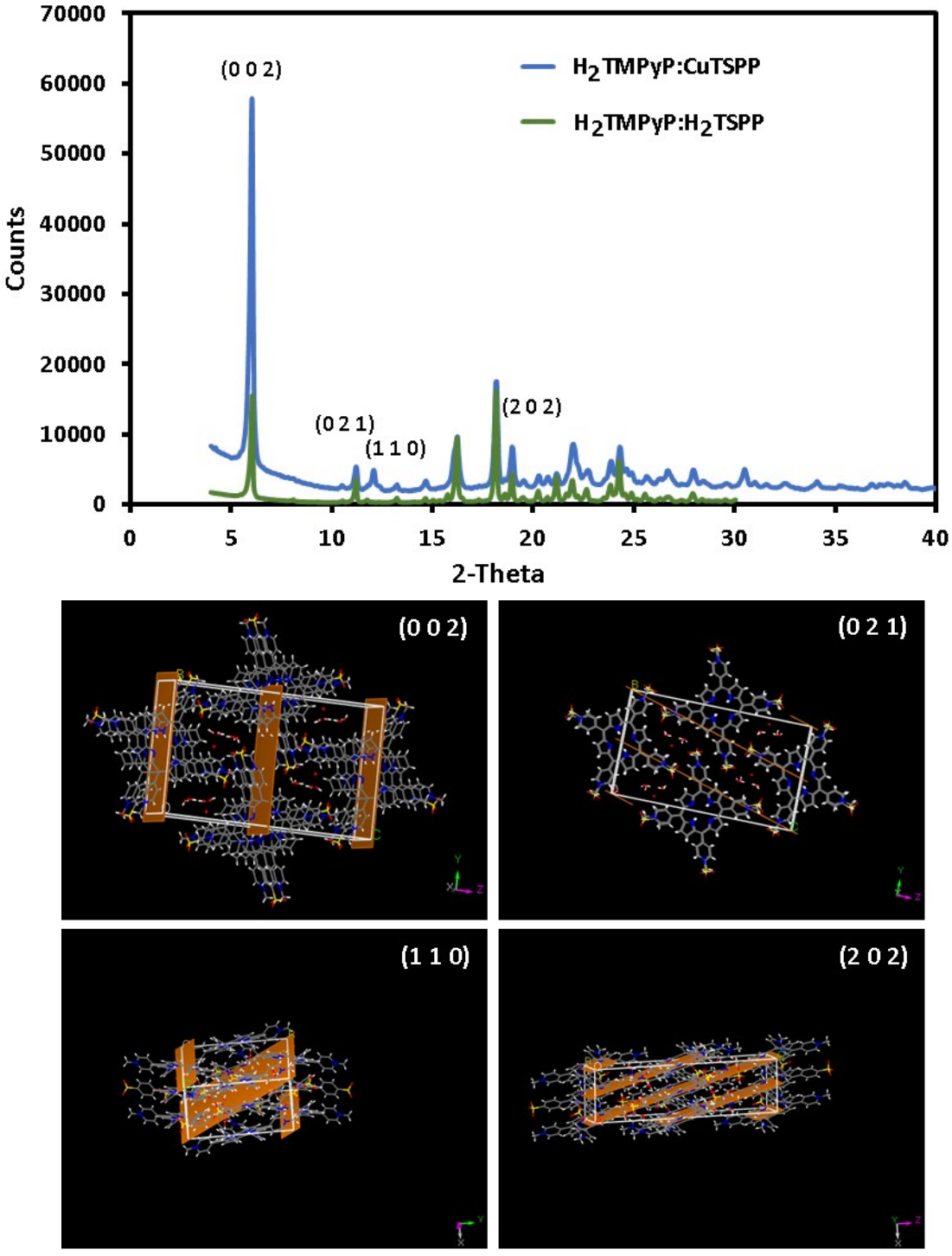

Fig. S5 Top figure compares peak intensities of the XRDs obtained from the metallated and free-base crystals. Although both patterns are nearly identical, the intensities of some peaks are different. This is particularly apparent for the case of the crystalline planes, shown in the lower figure, which include the (0 0 2), (0 2 1), (1 1 0), and (2 0 2) containing all or some of the tecton metal atoms which have a higher atomic scattering factor intense.

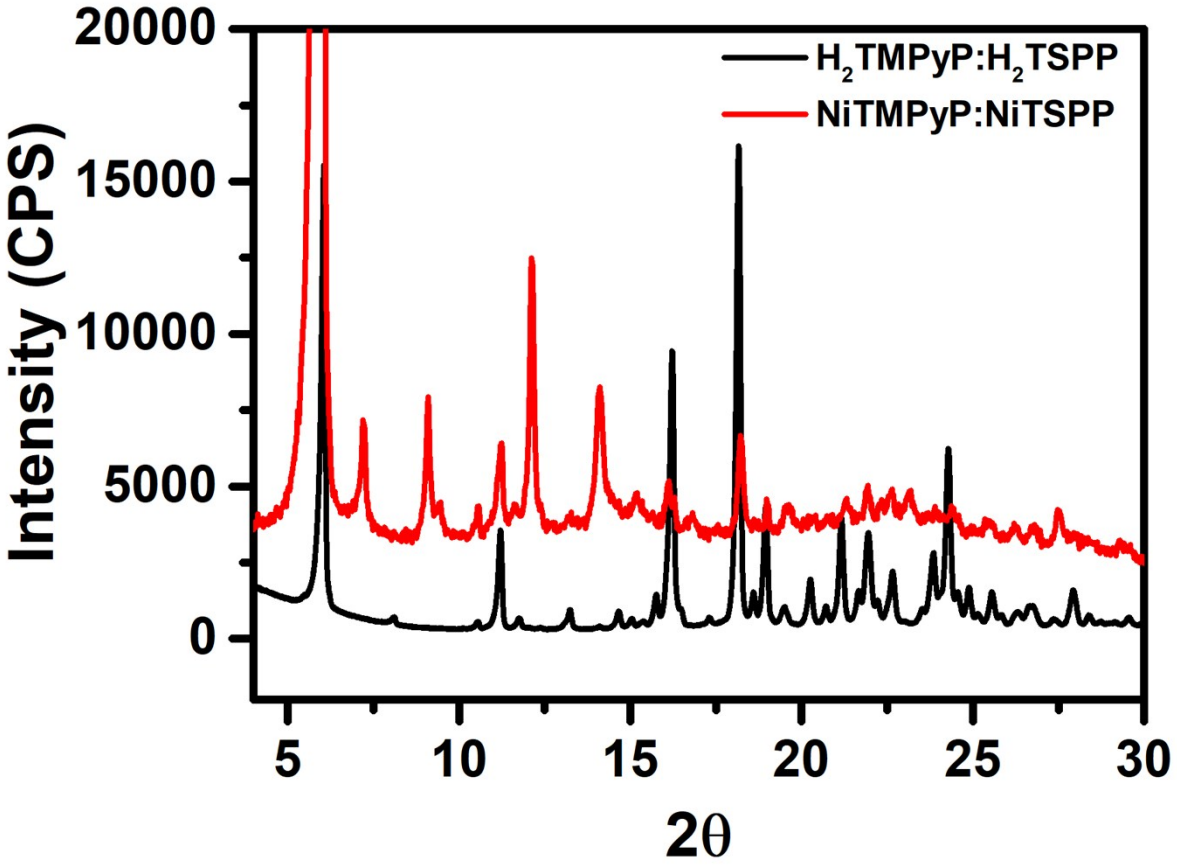

Fig. S6 Comparison of powder XRD patterns obtained from H_2TMPyP:H_2TSPP and NiTMPyP:NiTSPP crystals.

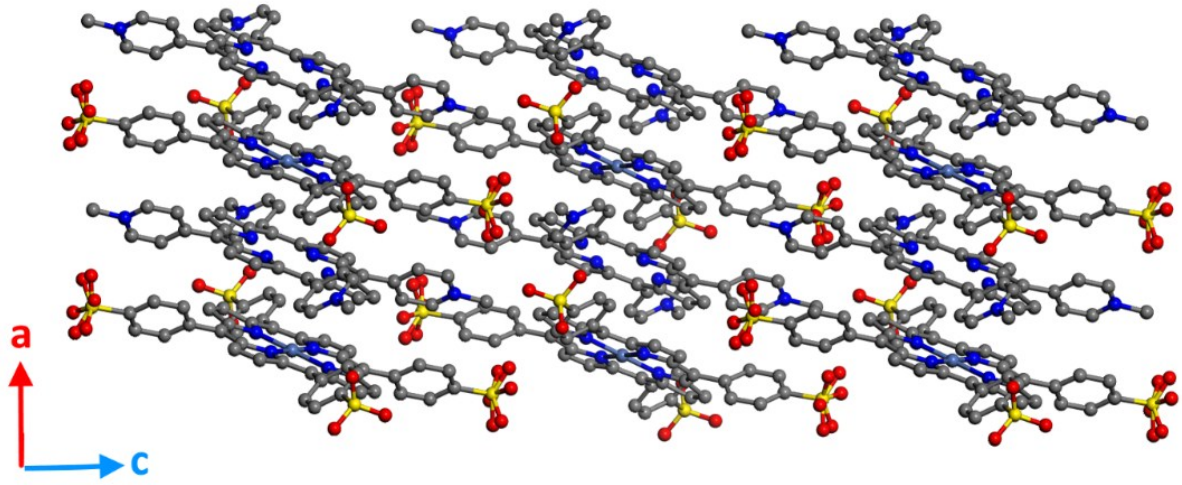

Fig. S7 Crystal structure of the H_2TMPyP:NiTSPP nanorods in the direction normal to the crystallographic *b* axis, showing alternating $[H_2TMPyP]^{4+}$ and $[NiTSPP]^{4-}$ porphyrin tectons within the columns. Color codes: blue, N; grey, C, yellow; S; red, O (hydrogens not shown). Waters within the columns are not shown.

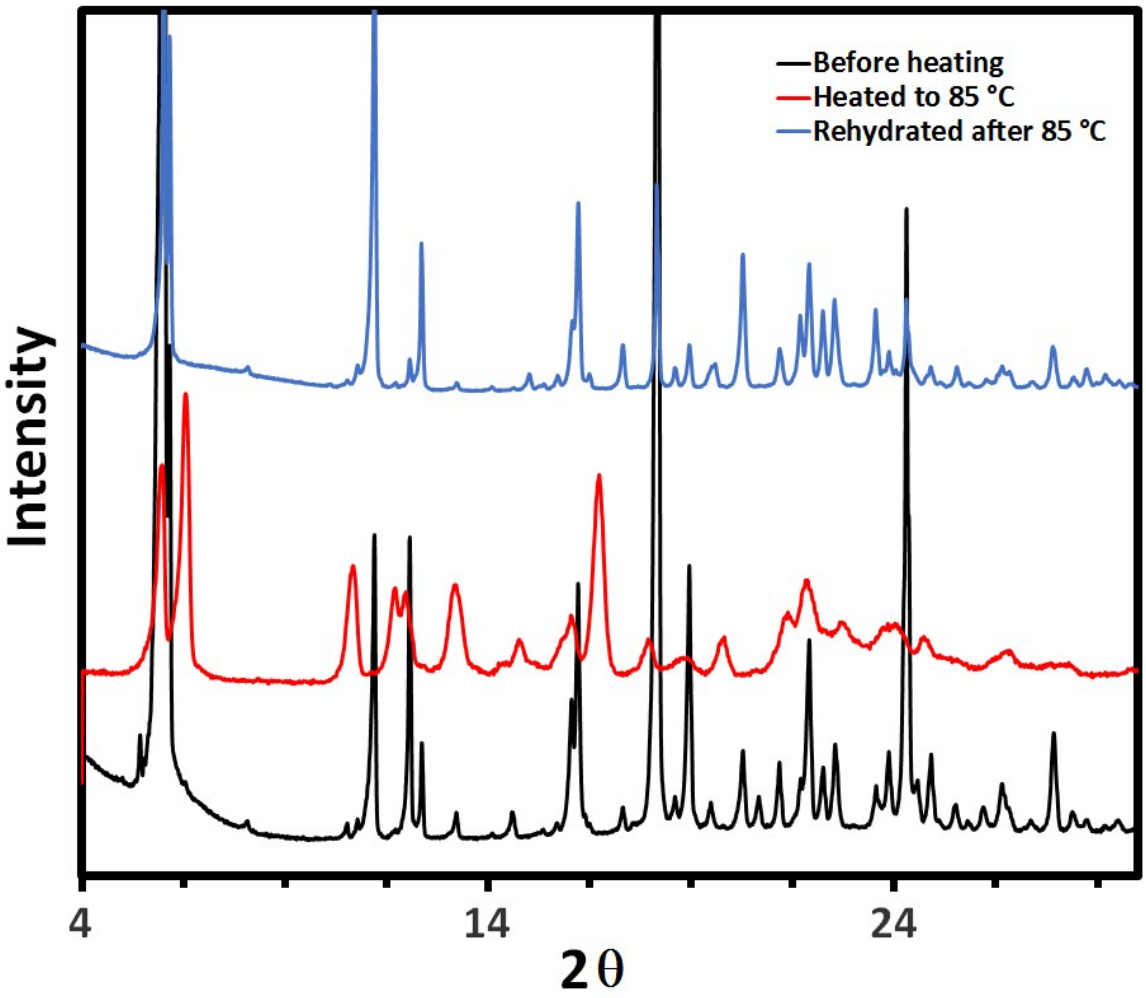

Fig. S8 Comparison of the powder XRD patterns obtained from a H_2TMPyP: NiTSPP sample before heating (black), after heating to 85 °C (red) and after rehydration of the crystals (blue).

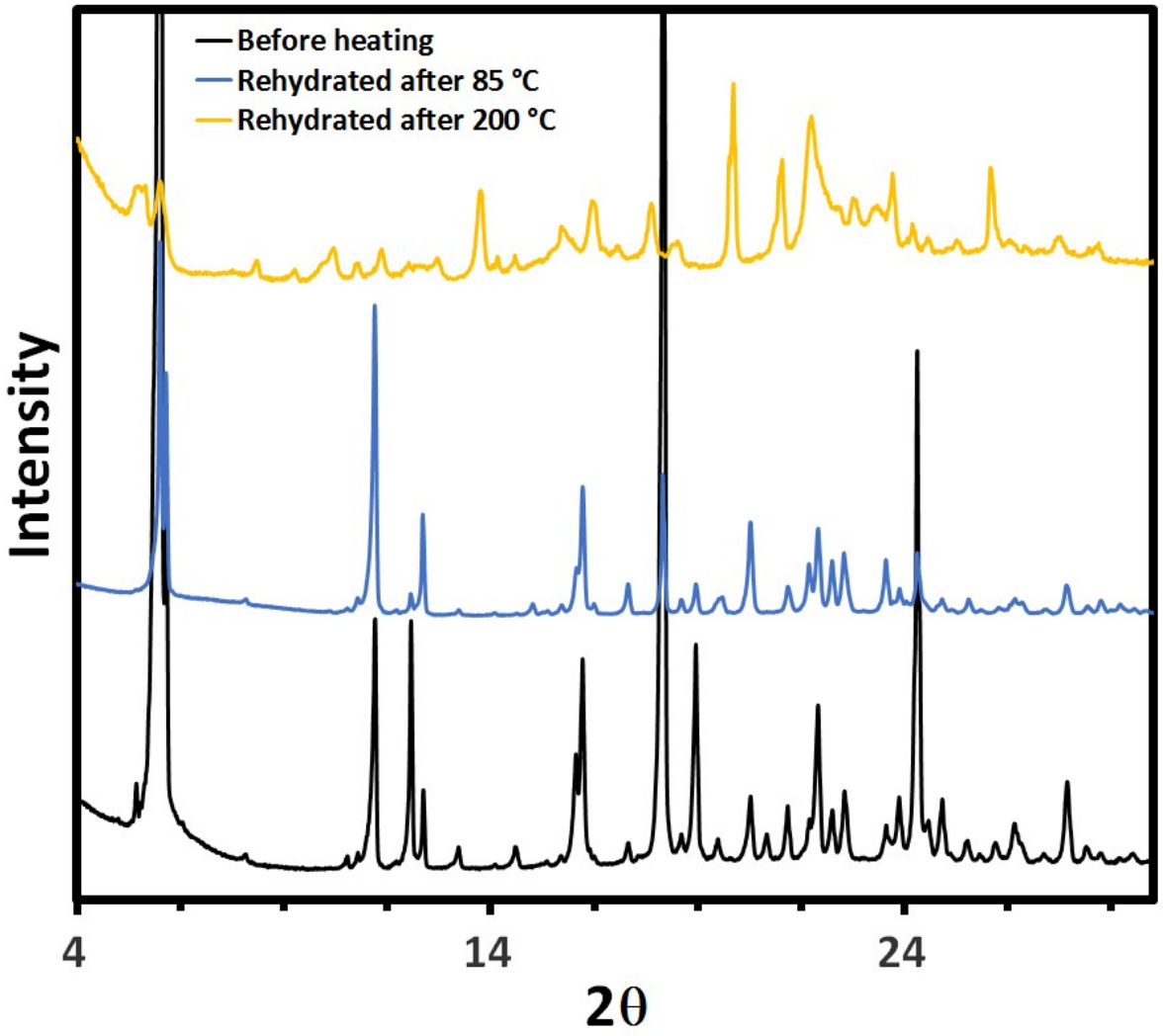

Fig. S9 Comparison of the powder XRD patterns obtained from a H_2TMPyP:NiTSPP sample before heating (black), after heating to 85 °C and rehydration (blue) and after heating to 200 °C and rehydration after rehydration of the crystals (yellow).

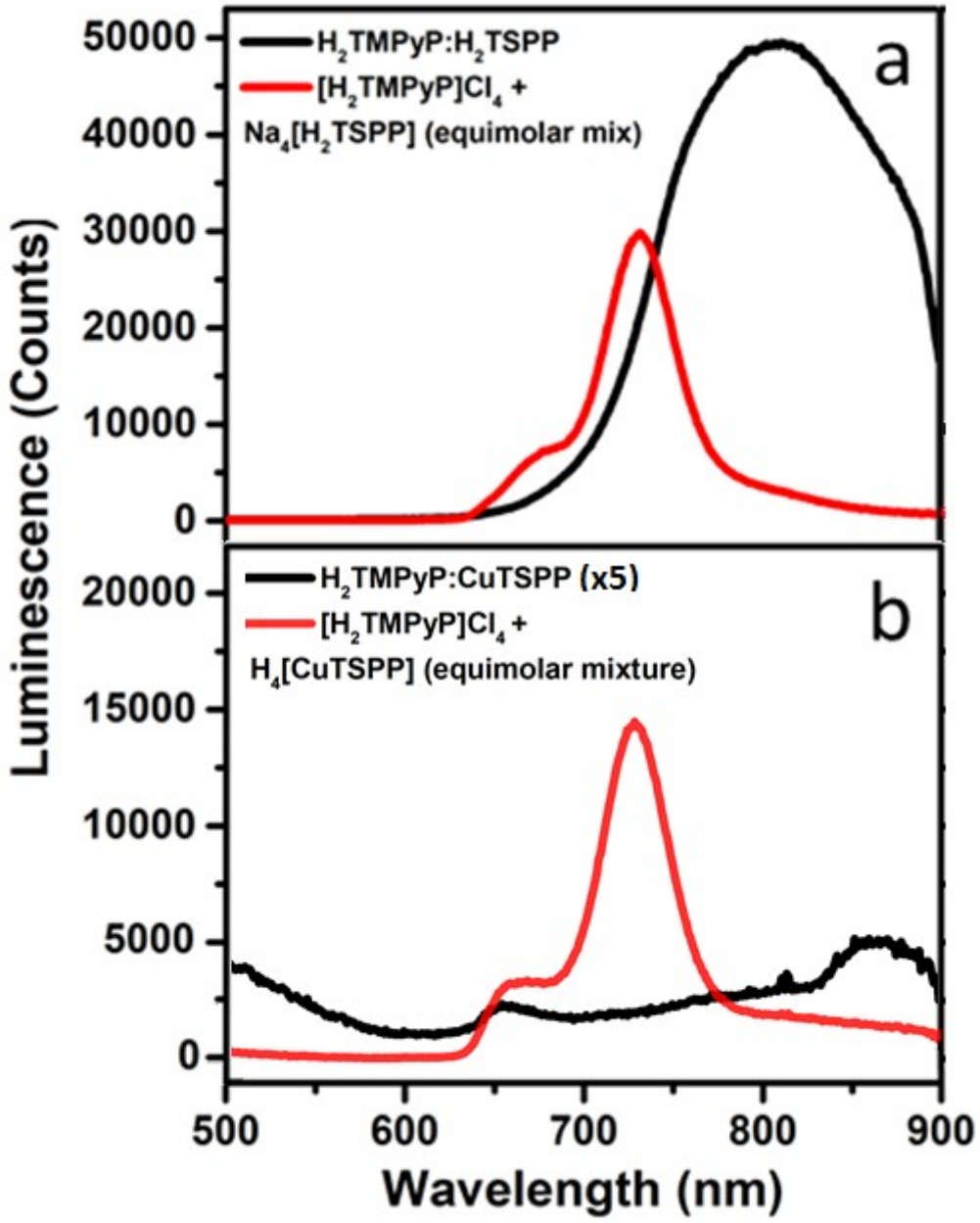

Fig. S10 Luminescence spectra of the free base (a) and Cu based (b) ISA crystals (black) and equimolar mixtures of the monomer starting materials (red).

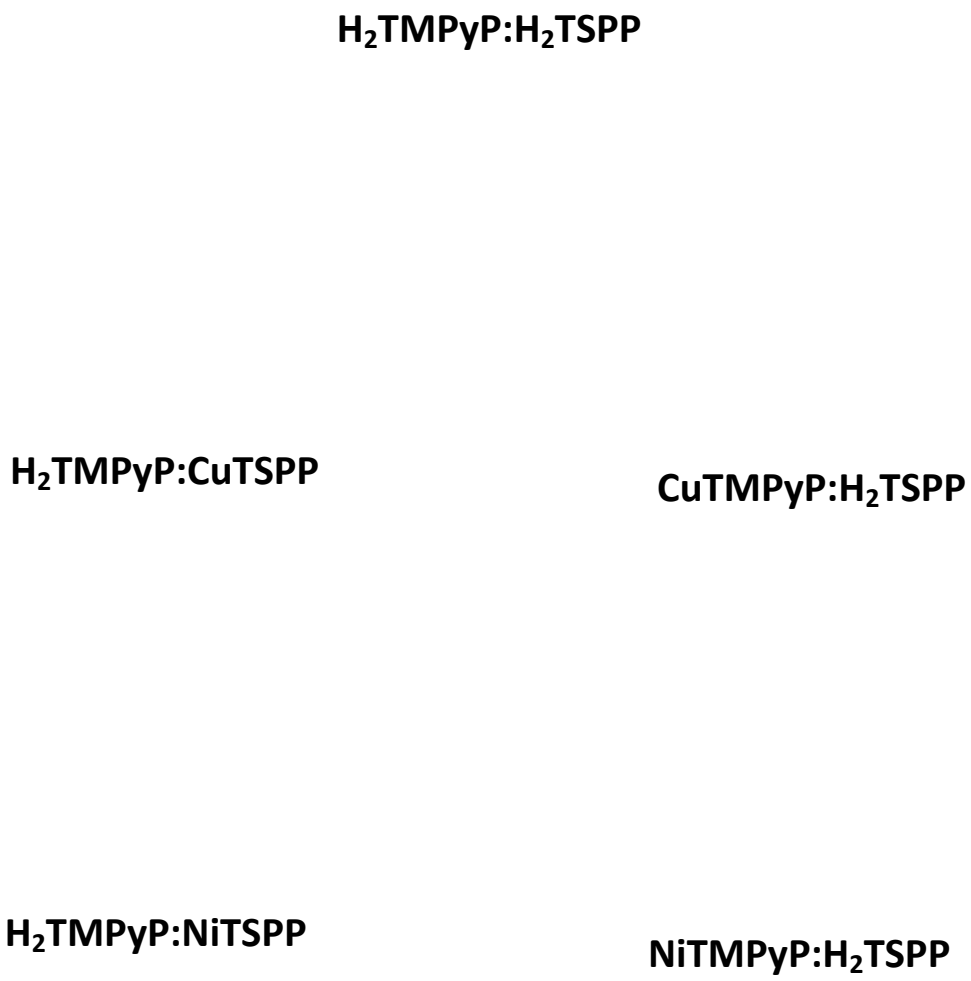

Fig. S11 Current-voltage characteristics of different ISA crystals acquired at 25 °C. Illumination curves were collected under 8 mW laser power.

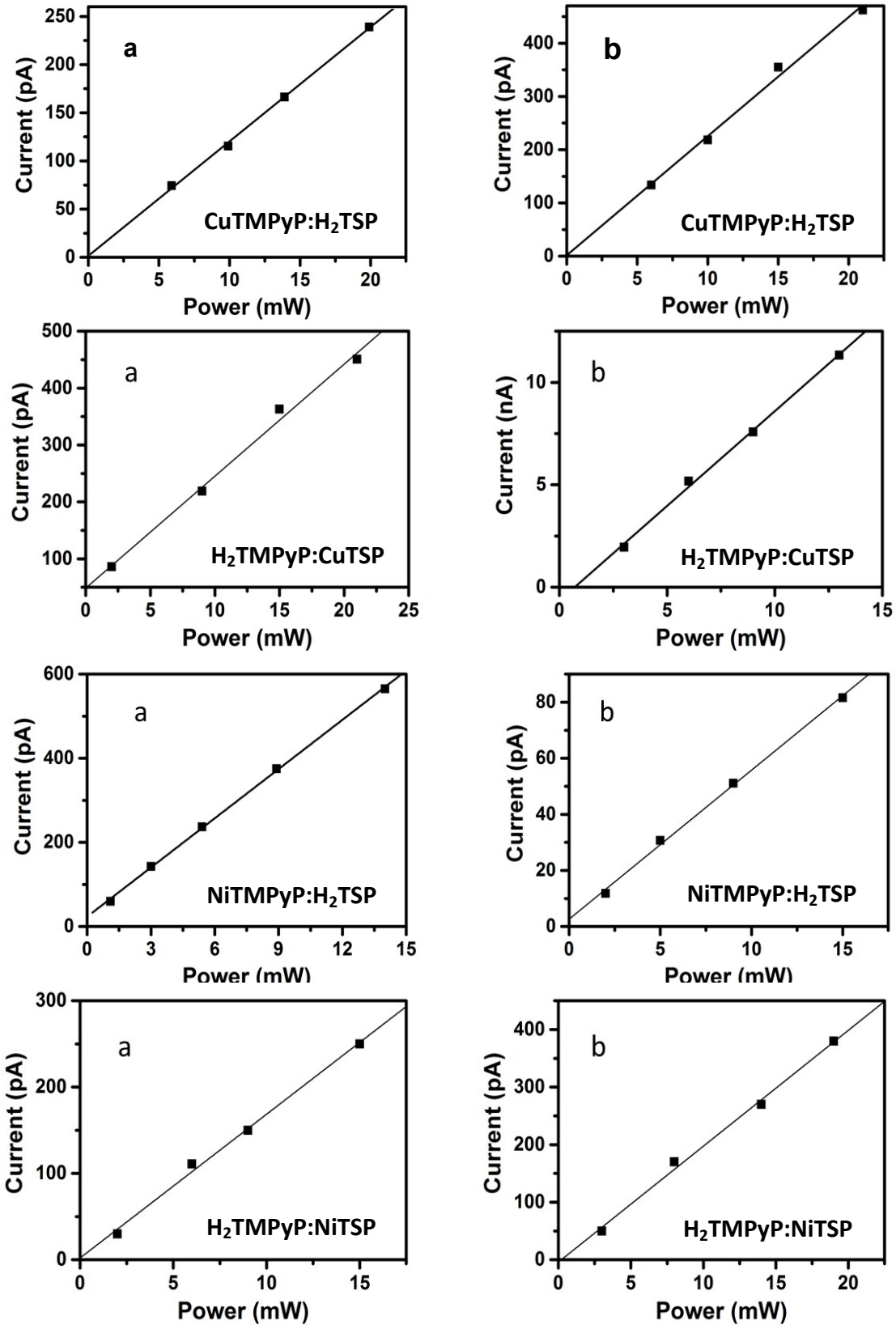

Fig. S12 Power dependence of photocurrent for copper and nickel ISAs with (a) 671 nm excitation and (b) 445 nm excitation.

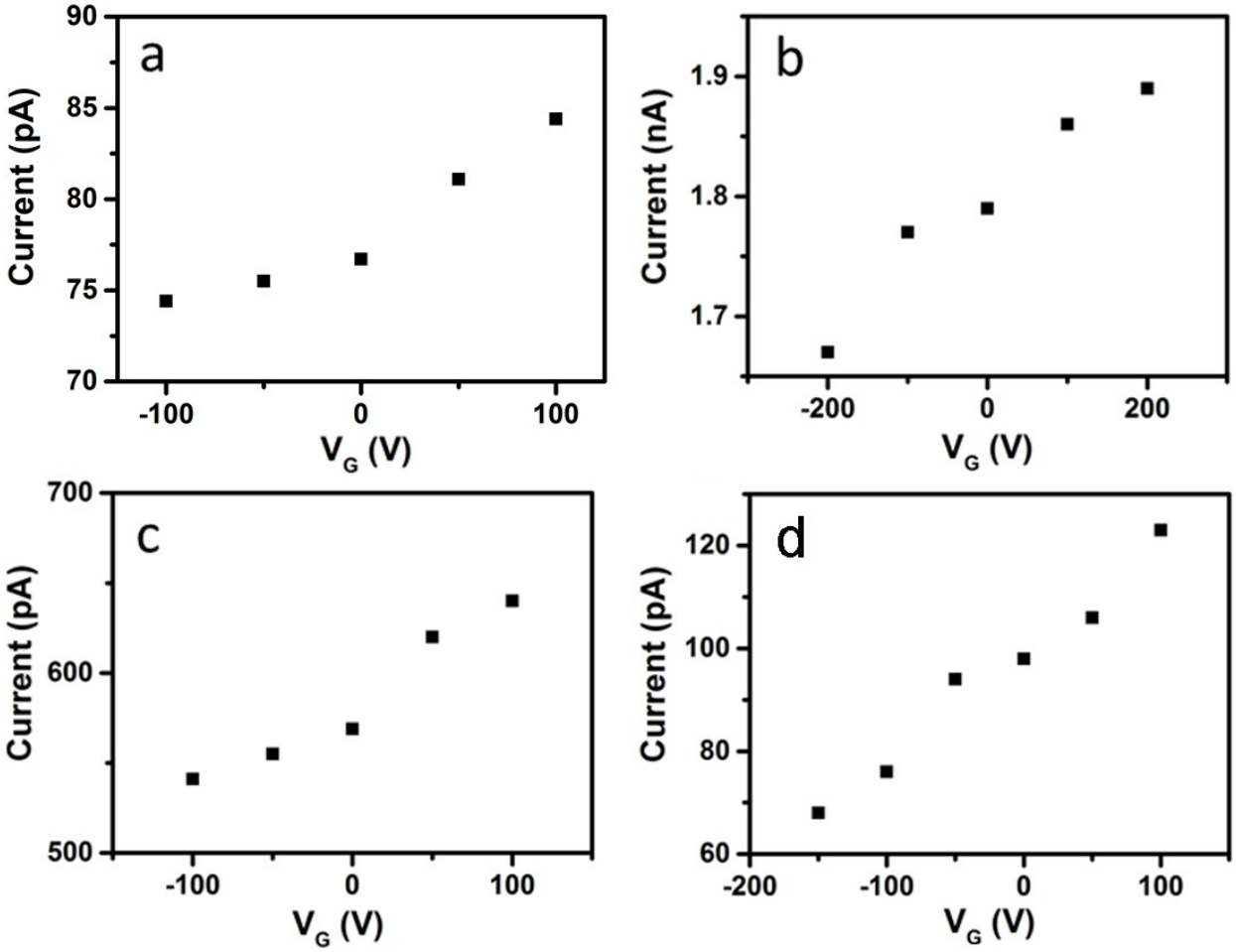

Fig. S13 Gate voltage dependence of the conductivity of (a) NiTMPyP:H_2TSPP, (b) H_2TMPyP:CuTSPP, (c) NiTMPyP:H_2TSPP and (d) H_2TMPyP:NiTSPP.

a

b

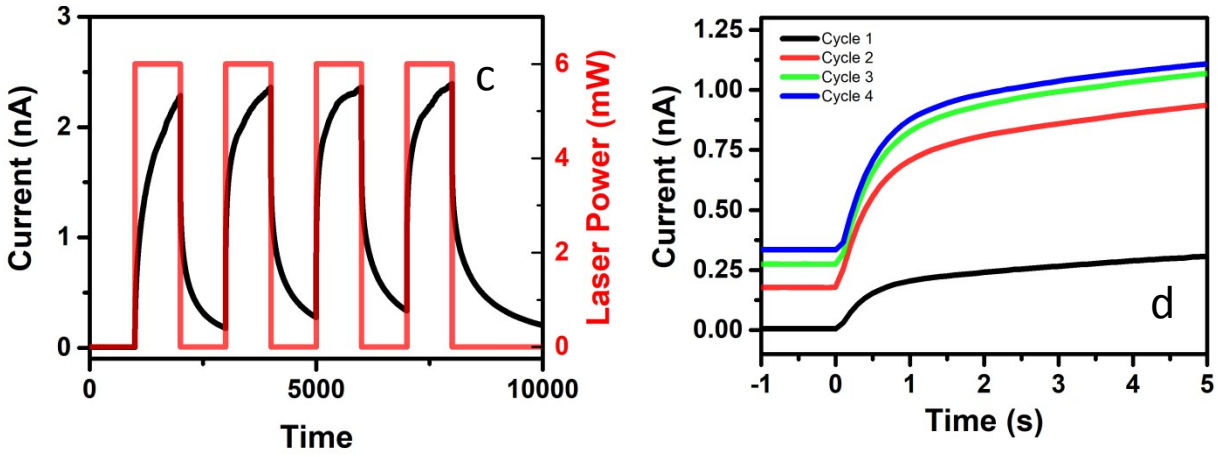

Fig. S14 H_2TMPyP:CuTSPP photoresponse under cycled Illumination with: (a) and (b) 406 nm laser light; (c) and (d) 671 nm laser light.

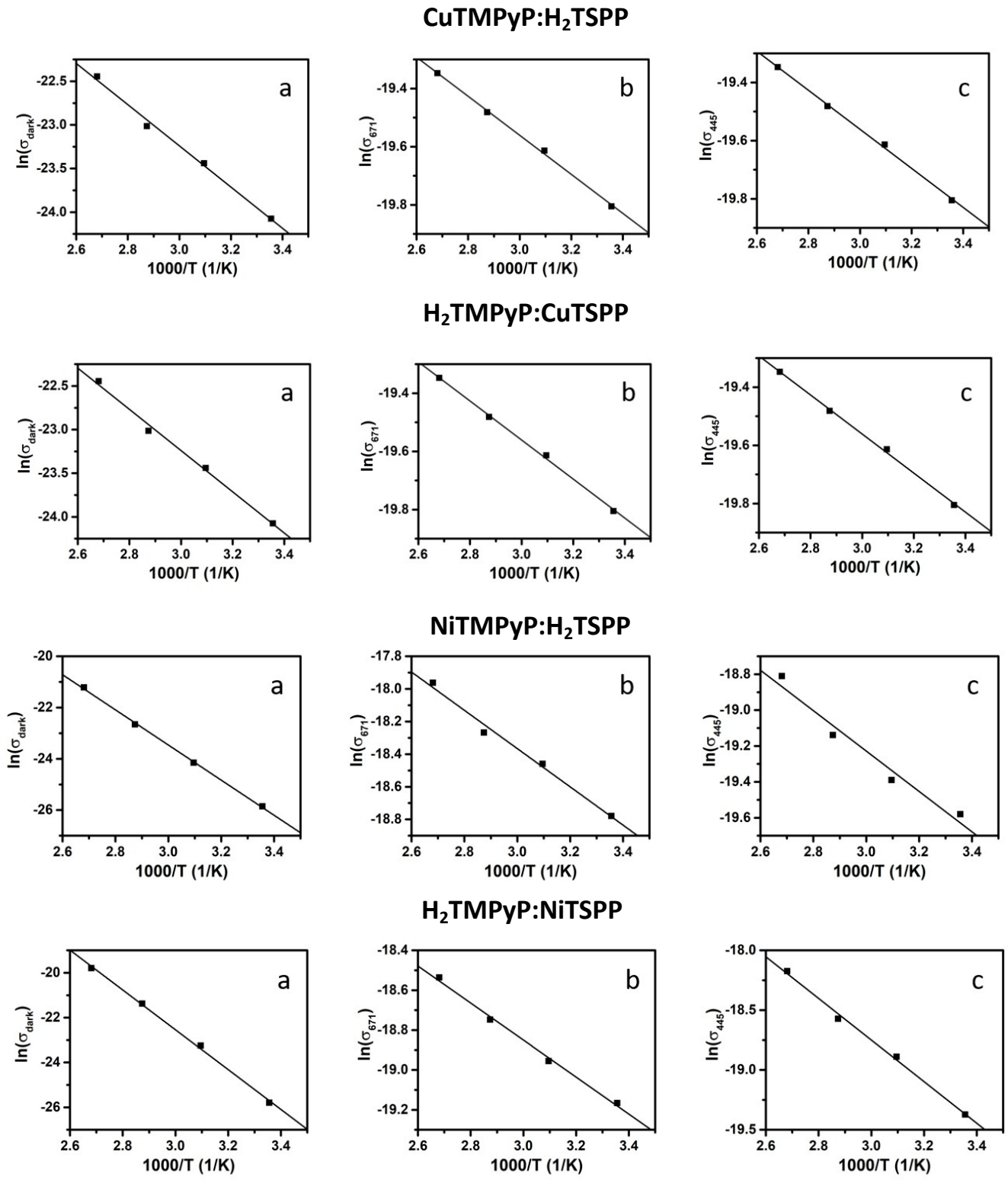

Fig. S15 Temperature dependence of the conductivity of ISA porphyrin rods (a) in the dark, (b) under 445 nm excitation and (c) under 671 nm excitation. All data was collected with a 5 V bias under 1 W·cm^{-2} illuminati

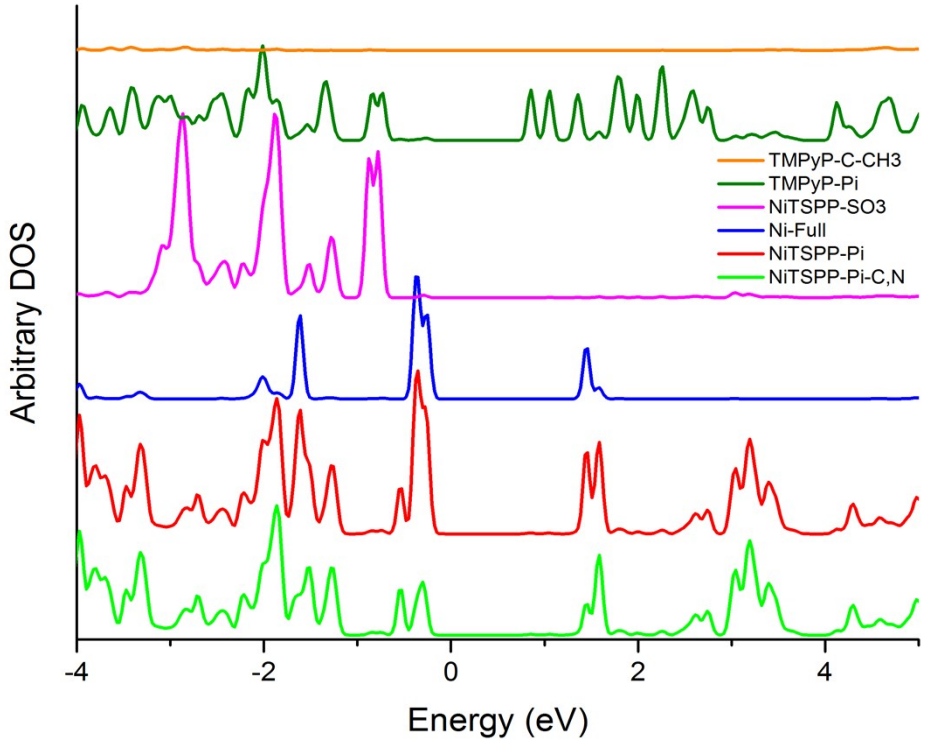

Fig. S16 Projected density of states (pDOS) of H_2TMPyP:NiTSPP crystal from DFT.

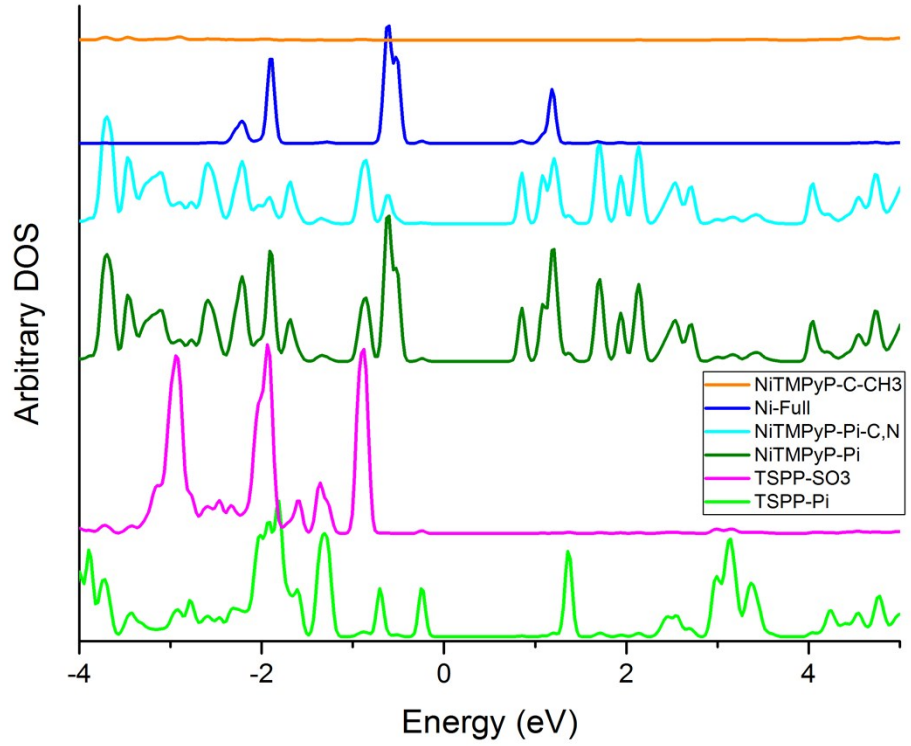

Fig. S17 Projected density of states (pDOS) of NiTMPyP:H_2TSPP crystal from DFT.

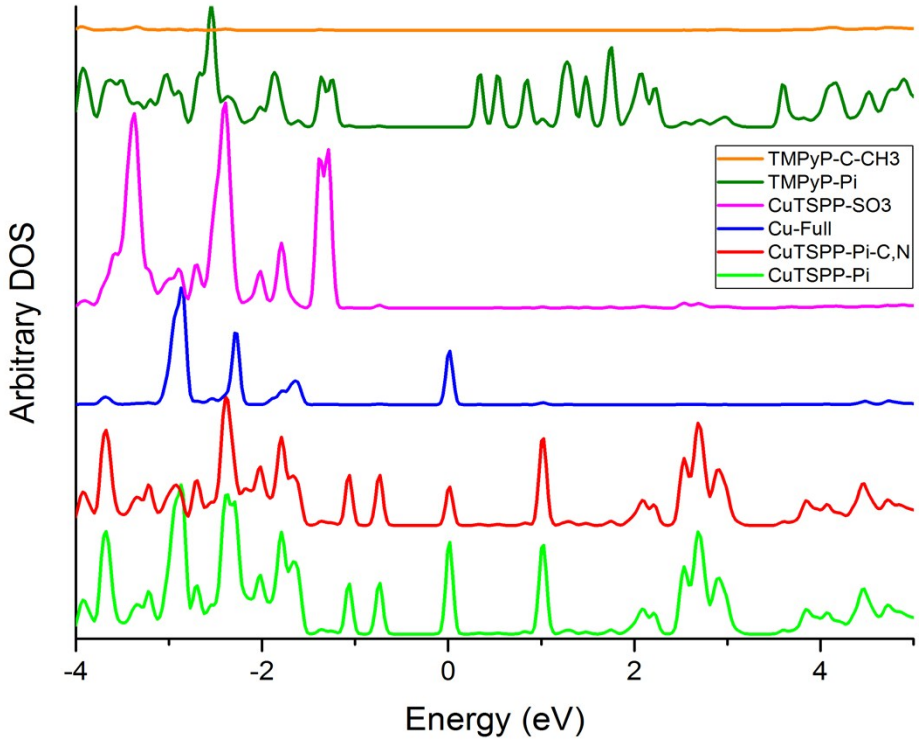

Fig. S18 Projected density of states (pDOS) of H_2TMPyP:CuTSPP crystal from DFT.

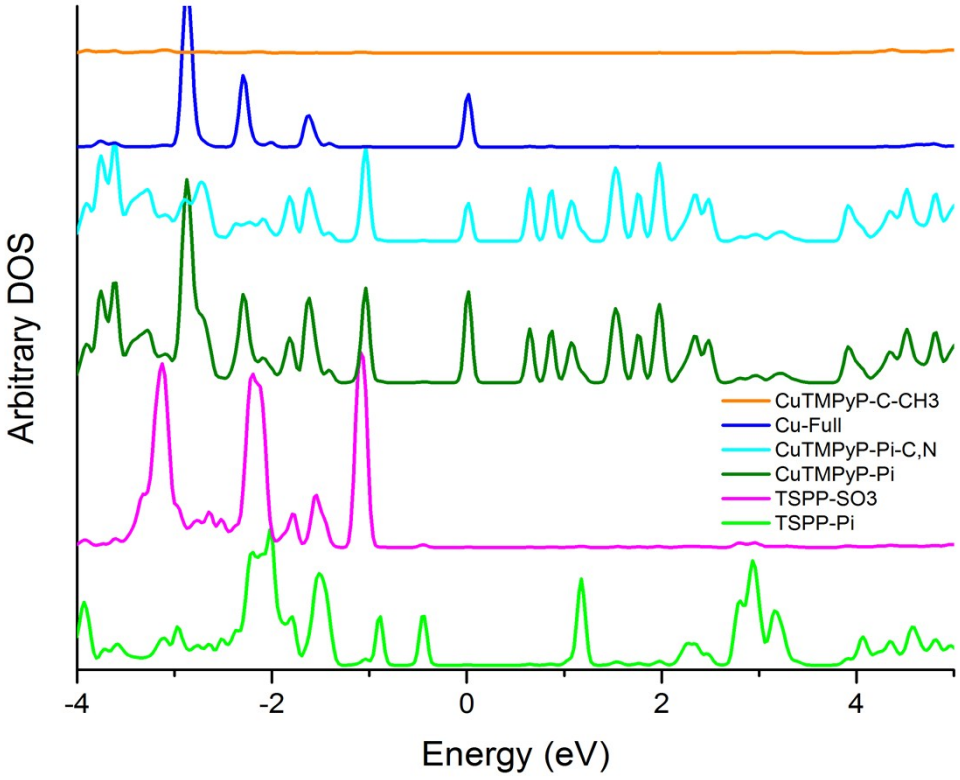

Fig. S19 Projected density of states (pDOS) of CuTMPyP:H_2TSPP crystal from DFT.

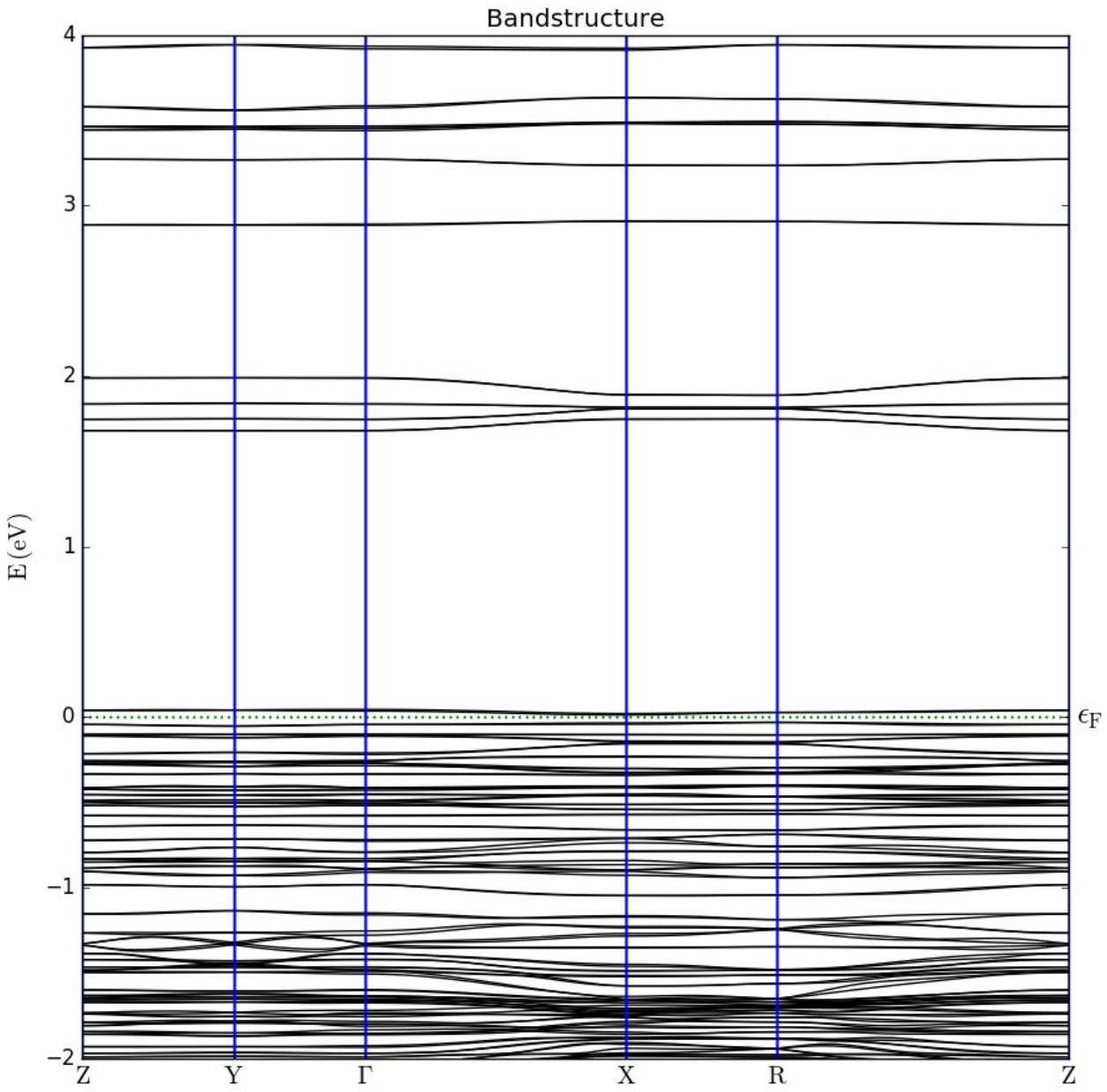

Fig. S20 Band structure of H_2TMPyP:NiTSPP crystal from EHTB. Fermi level (E_f) is located at zero. The high symmetry points the Brillouin zone are as follows, Ƭ = (0,0,0), Z = (0,0,0.5), Y = (0,0.5,0), X = (0.5,0,0), R = (0.5,0.5,0.5).

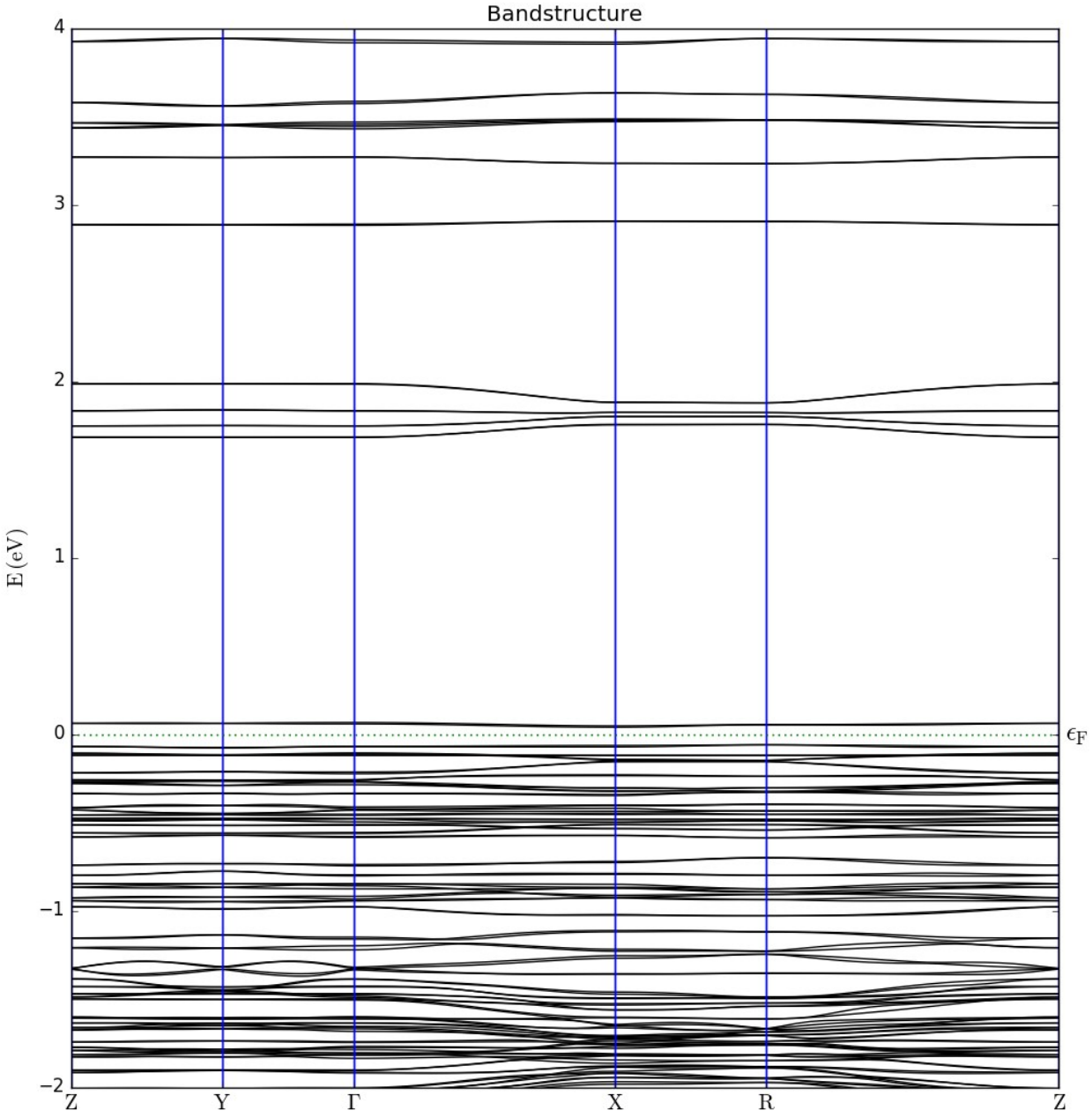

Fig. S21 Band structure of NiTMPyP:H_2TSPP crystal from EHTB. Fermi level (E_f) is located at zero. The high symmetry points the Brillouin zone are as follows, Ϝ = (0,0,0), Z = (0,0,0.5), Y = (0,0.5,0), X = (0.5,0,0), R = (0.5,0.5,0.5).

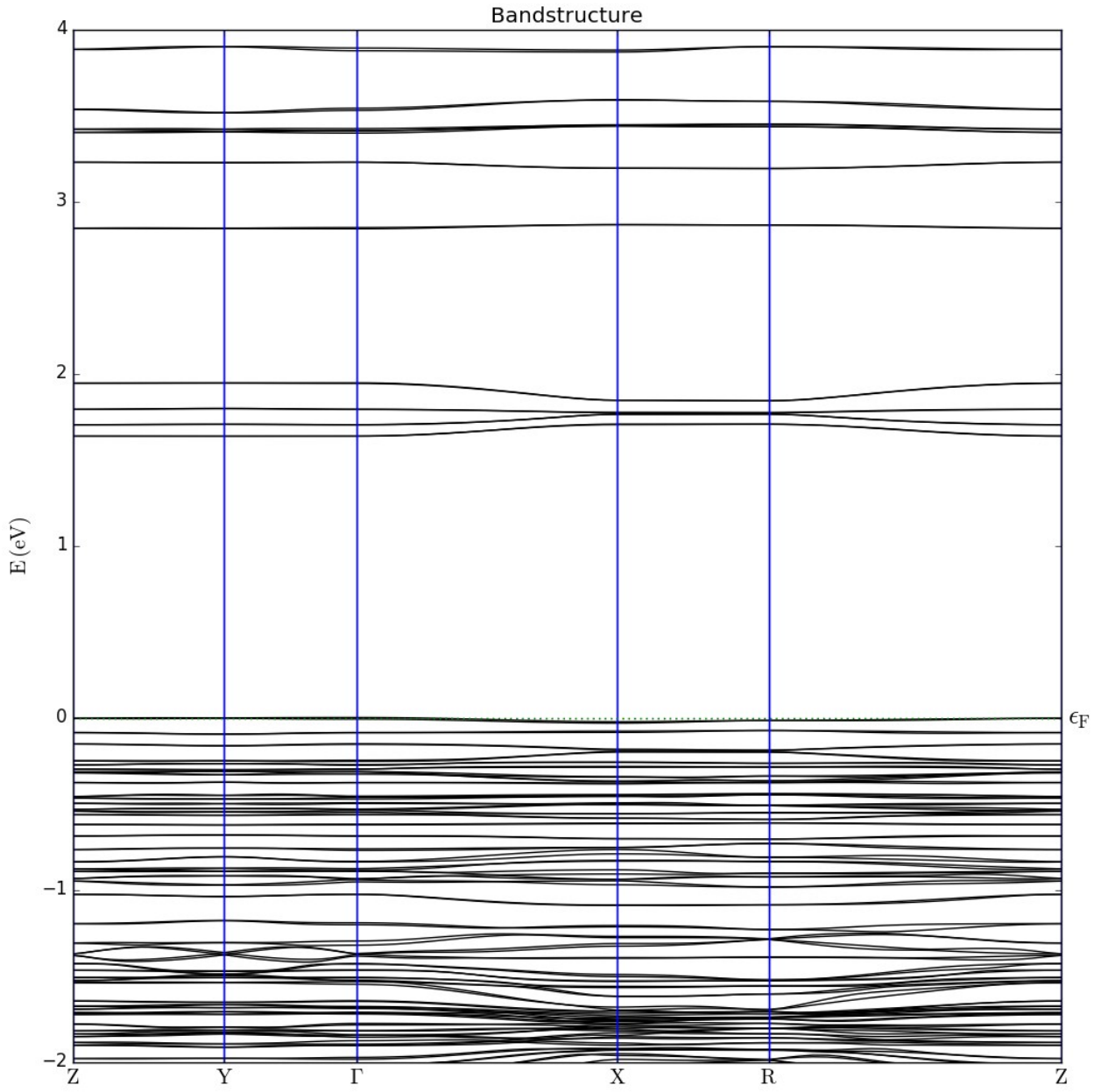

Fig. S22 Band structure of H_2TMPyP:CuTSPP crystal from EHTB. Fermi level (E_f) is located at zero. The high symmetry points the Brillouin zone are as follows, Ƭ = (0,0,0), Z = (0,0,0.5), Y = (0,0.5,0), X = (0.5,0,0), R = (0.5,0.5,0.5).

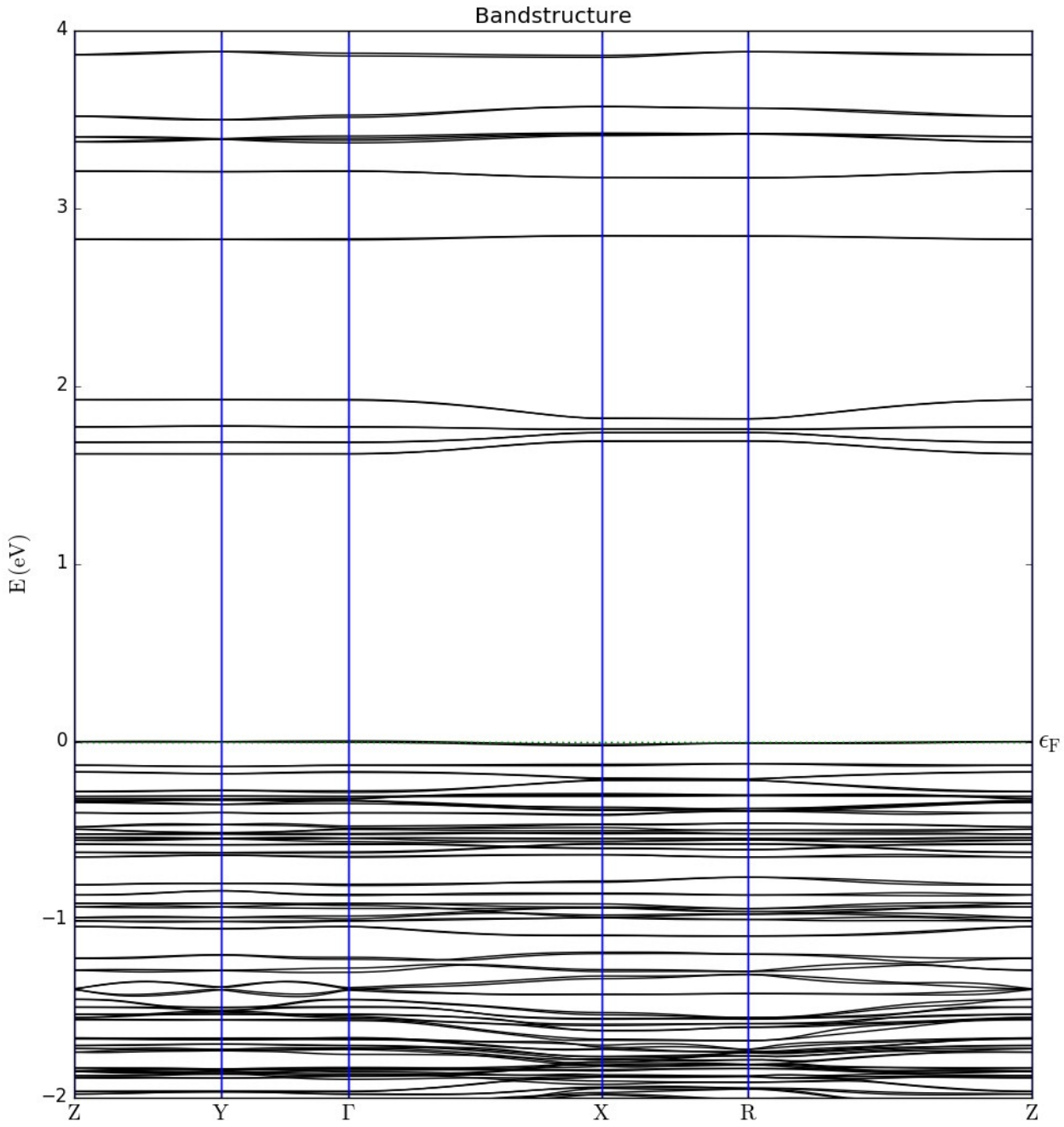

Fig. S23 Band structure of CuTMPyP:H_2TSPP crystal from EHTB. Fermi level (E_f) is located at zero. The high symmetry points the Brillouin zone are as follows, Ƭ = (0,0,0), Z = (0,0,0.5), Y = (0,0.5,0), X = (0.5,0,0), R = (0.5,0.5,0.5).

Resistivity Calculation.

$$\sigma = \frac{l}{AR} = \frac{Il}{VA}$$

R: resistance

V: sample bias

I: sample current

A: cross sectional area of crystalline rods

l: length of the IDE spacing

Photoresistivity Calculation.

$$\sigma = R\frac{A}{l} = \frac{VA}{Il}$$

R: resistance measured under 1.0 W/cm^2 illumination.

V: sample bias

I: sample current

A: cross sectional area of crystalline rods

l: length of the IDE spacing

The cross sectional area (A) was calculated using the aspect ratios of the ISA crystals obtained from microscopic data and the number of electrical connections the rods made with the IDE (from AFAM images). Length is the spacing between the IDE electrodes.

V and I were obtained from photoconductivity measurements.

XRD

The total exposure time was 48.73 hours with the temperature maintained at 100 ± 2 °C. The frames were integrated with the Bruker SAINT software package using a narrow-frame algorithm. The integration of the data using a monoclinic unit cell yielded a total of 52269 reflections to a maximum θ angle of 45.98° (0.82 Å resolution), of which 7520 were independent (average redundancy 6.951, completeness = 99.2%, R_{int} = 7.77%, R_{sig} = 5.59%) and 5963 (75.70%) were greater than 2σ(F2). The final cell constants are based on the refinement of the XYZ-centroid of 9922 reflections above 20 σ(I) with 5.280°<2θ<109.7°. Data were corrected for absorption effects using the Multi-Scan method (SADABS). The ratio of minimum to maximum transmission was 0.788. SHELXT-2014/15 software[8] was used for structure solutions and APEX3 v2016.1-0 (Bruker AXS, Inc.) was used for cell refinement computation.

Table S1. XPS based and calculated atomic ratios for 1:1 tecton stoichiometry for metalled porphyrin crystals.

Atomic ratios	H_2TMPyP:NiTSPP		H_2TMPyP:CuTSPP	
	Calculated	XPS	Calculated	XPS
S/N	0.33	0.35	0.33	0.33
Ni/N	0.083	0.076	--	--
Cu/N	--	--	0.083	0.080

Table S2. Data collection and structure refinement parameters from XRD experiment of H_2TMPyP:NiTSPP nanorods	
Parameter Type	**Parameter Value**
Teta range for data collection	2.64 to 54.98°
Index ranges	-10≤h≤8, -19≤k≤19, -35≤l≤34
Reflections collected	52269
Independent reflections	7520 [R_{int} = 0.0777]
Coverage of independent reflections	99.2%
Absorption correction	Multi-Scan
Refinement method	Full-matrix least squares on F^2
Refinement program	SHELXL-2014/7 (Sheldrick)[9]
Function minimized	$\sum w(F_O^2-F_C^2)^2$
Data / restrains / parameters	7520 / 117 / 650
Goodness-of-fit on F^2	1.061
Δ/σ_{max}	0.005
Final R indices	5693 data; I>2σ(I) R1 = 0.0542, wR2 = 0.01444 All data R1 = 0.0792, wR2 = 0.1574
Weighting scheme	$W = 1/[\sigma^2(F_O^2)+(0.0832P)^2+3.4525P]$ Where $P = (F_O^2+2F_C^2)/3$
Largest diff. peak and hole	1.052 and -0.610 eÅ^{-3}
R.M.S. deviation from mean	0.078 eÅ^{-3}

Table S3. Atomic coordinates and equivalent isotropic atomic displacement parameters (Å²) for H_2TMPyP:NiTSPP crystals				
	x/a	**y/b**	**z/c**	**U(eq)**
Ni1	0.5	0.0	0.0	0.01846(17)
S1	0.78314(11)	0.46319(5)	0.90777(3)	0.0330(2)
S2	0.28516(12)	0.82066(6)	0.30126(3)	0.0398(2)
O1	0.8371(4)	0.47518(14)	0.86152(9)	0.0452(7)
O2	0.6401(3)	0.41353(13)	0.90986(9)	0.0414(6)
O3	0.9128(3)	0.43635(13)	0.93901(9)	0.0397(6)
O4	0.1220(3)	0.78982(18)	0.30155(9)	0.0442(8)
O5	0.4040(3)	0.75778(18)	0.31138(9)	0.0483(8)
O6	0.3169(4)	0.89220(19)	0.32988(9)	0.0549(9)
O4A	0.1570(17)	0.8691(10)	0.3174(6)	0.066(12)
O5A	0.431(2)	0.8339(9)	0.3278(9)	0.047(10)
O6A	0.2489(15)	0.7362(9)	0.2965(9)	0.072(11)
N1	0.5918(3)	0.95002(14)	0.94598(8)	0.0214(5)
N2	0.5110(3)	0.89450(14)	0.03190(8)	0.0202(5)
C1	0.6315(4)	0.98732(17)	0.90537(10)	0.0212(6)
C2	0.7117(4)	0.93161(18)	0.87649(10)	0.0249(7)
C3	0.7165(4)	0.85904(19)	0.89779(10)	0.0257(7)
C4	0.6394(4)	0.86942(17)	0.94016(10)	0.0217(6)
C5	0.6186(4)	0.80620(17)	0.97147(10)	0.0219(7)
C6	0.5632(4)	0.81986(17)	0.01497(10)	0.0219(6)
C7	0.5529(4)	0.75750(18)	0.04934(10)	0.0245(7)
C8	0.4988(4)	0.79280(18)	0.08710(10)	0.0244(7)
C9	0.4690(4)	0.87724(17)	0.07650(10)	0.0210(6)
C10	0.6570(4)	0.72077(17)	0.95678(10)	0.0224(7)
C11	0.5853(4)	0.68850(18)	0.91634(10)	0.0228(7)
C12	0.6211(4)	0.60995(18)	0.90183(10)	0.0249(7)
C13	0.7296(4)	0.56227(17)	0.92759(11)	0.0258(7)
C14	0.7996(4)	0.59247(19)	0.96818(11)	0.0276(7)
C15	0.7635(4)	0.67076(18)	0.98243(11)	0.0260(7)
C16	0.4034(4)	0.93198(17)	0.10690(10)	0.0216(7)
C17	0.3712(4)	0.90472(18)	0.15452(10)	0.0232(7)
C18	0.2814(4)	0.83433(19)	0.16295(11)	0.0272(7)
C19	0.2545(4)	0.8082(2)	0.20719(11)	0.0308(8)
C20	0.3162(4)	0.8541(2)	0.24410(11)	0.0306(8)
C21	0.4029(4)	0.9245(2)	0.23685(11)	0.0300(7)
C22	0.4316(4)	0.94880(19)	0.19256(10)	0.0263(7)
N3	0.9068(3)	0.44750(14)	0.55725(8)	0.0231(6)
N4	0.0084(3)	0.60957(14)	0.53562(8)	0.0229(6)
N5	0.8124(3)	0.62882(16)	0.74806(8)	0.0281(6)

N6	0.2263(3)	0.93522(15)	0.43065(9)	0.0276(6)
C00Z	0.1202(4)	0.69308(17)	0.47386(10)	0.0232(7)
C23	0.8586(4)	0.36730(17)	0.55977(10)	0.0231(7)
C24	0.7820(4)	0.35464(19)	0.60255(10)	0.0272(7)
C25	0.7884(4)	0.42610(18)	0.62570(11)	0.0266(7)
C26	0.8690(4)	0.48448(18)	0.59746(10)	0.0233(7)
C27	0.9014(4)	0.56668(18)	0.60932(10)	0.0229(7)
C28	0.9615(4)	0.62513(17)	0.57946(10)	0.0226(7)
C29	0.9872(4)	0.71068(18)	0.58941(10)	0.0239(7)
C30	0.0474(4)	0.74516(17)	0.55201(10)	0.0232(7)
C31	0.0627(4)	0.68172(17)	0.51782(10)	0.0217(6)
C32	0.8724(4)	0.59066(17)	0.65739(10)	0.0217(7)
C33	0.9367(4)	0.5443(2)	0.69430(11)	0.0282(7)
C34	0.9047(4)	0.5644(2)	0.73861(11)	0.0302(7)
C35	0.7522(4)	0.67612(19)	0.71367(11)	0.0271(7)
C36	0.7806(4)	0.65872(18)	0.66871(10)	0.0237(7)
C37	0.7727(4)	0.6468(2)	0.79594(11)	0.0358(8)
C38	0.1581(4)	0.77841(17)	0.45968(10)	0.0226(7)
C39	0.2616(4)	0.82934(18)	0.48546(11)	0.0247(7)
C40	0.2942(4)	0.90660(19)	0.47008(11)	0.0278(7)
C41	0.1233(4)	0.88909(19)	0.40565(11)	0.0279(7)
C42	0.0880(4)	0.81092(18)	0.41933(11)	0.0266(7)
C43	0.2688(5)	0.0177(2)	0.41351(13)	0.0367(9)
O7	0.361(4)	0.6133(14)	0.2618(7)	0.108(9)
O7A	0.3083(13)	0.5645(7)	0.2338(4)	0.107(4)
O8	0.5795(5)	0.6499(2)	0.25828(11)	0.0582(9)
O9	0.5970(4)	0.64467(18)	0.16331(11)	0.0591(8)
O10	0.9407(4)	0.63950(18)	0.17811(11)	0.0628(9)
O11	0.9253(5)	0.6444(2)	0.27533(11)	0.0747(10)
*U(eq) is defined as one third of the trace of the orthogonalized U_{ij} tensor.				

Table S4. Interatomic distances (Å) in H_2TMPyP:NiTSPP crystal structure			
Ni1-N1	1.960(2)	Ni1-N1	1.960(2)
Ni1-N2	1.963(2)	Ni1-N2	1.963(2)
S1-O2	1.446(3)	S1-O3	1.453(3)
S1-O1	1.454(3)	S1-C13	1.786(3)
S2-O6A	1.421(15)	S2-O4A	1.425(15)
S2-O5A	1.429(15)	S2-O4	1.450(3)
S2-O5	1.450(3)	S2-O6	1.457(3)
S2-C20	1.785(3)	N1-C1	1.385(4)
N1-C4	1.391(4)	N2-C9	1.391(4)
N2-C6	1.395(4)	C1-C16	1.397(4)
C1-C2	1.427(4)	C2-C3	1.341(4)
C2-H2	0.95	C3-C4	1.427(4)
C3-H3	0.95	C4-C5	1.396(4)
C5-C6	1.387(4)	C5-C10	1.501(4)
C6-C7	1.436(4)	C7-C8	1.339(4)
C7-H7	0.95	C8-C9	1.436(4)
C8-H8	0.95	C9-C16	1.389(4)
C10-C15	1.401(4)	C10-C11	1.404(4)
C11-C12	1.390(4)	C11-H11	0.95
C12-C13	1.391(4)	C12-H12	0.95
C13-C14	1.390(5)	C14-C15	1.385(4)
C14-H14	0.95	C15-H15	0.95
C16-C1	1.396(4)	C16-C17	1.495(4)
C17-C22	1.400(4)	C17-C18	1.401(4)
C18-C19	1.387(4)	C18-H18	0.95
C19-C20	1.394(5)	C19-H19	0.95
C20-C21	1.381(5)	C21-C22	1.383(4)
C21-H21	0.95	C22-H22	0.95
N3-C26	1.369(4)	N3-C23	1.376(4)
N3-H3A	0.88	N4-C31	1.374(4)
N4-C28	1.377(4)	N4-H4	0.88
N5-C34	1.341(4)	N5-C35	1.348(4)
N5-C37	1.479(4)	N6-C41	1.337(4)
N6-C40	1.345(4)	N6-C43	1.488(4)
C00Z-C31	1.401(4)	C00Z-C23	1.409(4)
C00Z-C38	1.495(4)	C23-C00Z	1.410(4)
C23-C24	1.441(4)	C24-C25	1.351(4)
C24-H24	0.95	C25-C26	1.445(4)
C25-H25	0.95	C26-C27	1.413(4)
C27-C28	1.400(4)	C27-C32	1.486(4)
C28-C29	1.445(4)	C29-C30	1.344(4)

C29-H29	0.95	C30-C31	1.450(4)
C30-H30	0.95	C32-C36	1.399(4)
C32-C33	1.406(4)	C33-C34	1.371(4)
C33-H33	0.95	C34-H34	0.95
C35-C36	1.373(4)	C35-H35	0.95
C36-H36	0.95	C37-H37A	0.98
C37-H37B	0.98	C37-H37C	0.98
C38-C39	1.397(4)	C38-C42	1.398(4)
C39-C40	1.373(4)	C39-H39	0.95
C40-H40	0.95	C41-C42	1.376(4)
C41-H41	0.95	C42-H42	0.95
C43-H43A	0.98	C43-H43B	0.98
C43-H43C	0.98	O7-H7A	0.9584(11)
O7-H7B	0.9584(11)	O7A-H7C	0.9584(11)
O7A-H7D	0.9584(11)	O8-H8A	0.9586(11)
O8-H8B	0.9585(10)	O9-H9A	0.9585(11)
O9-H9B	0.9584(11)	O10-H10A	0.9585(11)
O10-H10B	0.9585(11)	O11-H11A	0.9586(11)
O11-H11B	0.9585(10)		

Table S5. Bond angles (°) for H_2TMPyP:NiTSPP crystal structure. The anisotropic atomic displacement factor exponent takes the form: $-2\pi^2[h^2 a^{*2} U_{11} + ... + 2 h k a^* b^* U_{12}]$			
N1-Ni1-N1	180.0	N1-Ni1-N2	90.11(10)
N1-Ni1-N2	89.89(10)	N1-Ni1-N2	89.89(10)
N1-Ni1-N2	90.11(10)	N2-Ni1-N2	180.0
O2-S1-O3	113.31(15)	O2-S1-O1	113.71(16)
O3-S1-O1	111.94(17)	O2-S1-C13	106.27(15)
O3-S1-C13	105.11(15)	O1-S1-C13	105.62(14)
O6A-S2-O4A	114.5(8)	O6A-S2-O5A	111.9(9)
O4A-S2-O5A	111.5(10)	O4-S2-O5	112.54(18)
O4-S2-O6	115.12(19)	O5-S2-O6	110.37(19)
O6A-S2-C20	104.2(11)	O4A-S2-C20	106.1(8)
O5A-S2-C20	108.0(12)	O4-S2-C20	106.52(16)
O5-S2-C20	106.50(16)	O6-S2-C20	105.05(17)
C1-N1-C4	103.6(2)	C1-N1-Ni1	128.23(19)
C4-N1-Ni1	128.1(2)	C9-N2-C6	104.3(2)
C9-N2-Ni1	127.90(19)	C6-N2-Ni1	127.8(2)
N1-C1-C16	125.6(3)	N1-C1-C2	110.9(2)
C16-C1-C2	123.4(3)	C3-C2-C1	107.4(3)
C3-C2-H2	126.3	C1-C2-H2	126.3
C2-C3-C4	106.9(3)	C2-C3-H3	126.6
C4-C3-H3	126.6	N1-C4-C5	125.4(3)
N1-C4-C3	111.1(3)	C5-C4-C3	123.5(3)
C6-C5-C4	122.3(3)	C6-C5-C10	119.6(3)
C4-C5-C10	118.1(3)	C5-C6-N2	125.9(3)
C5-C6-C7	123.8(3)	N2-C6-C7	110.3(3)
C8-C7-C6	107.5(3)	C8-C7-H7	126.3
C6-C7-H7	126.3	C7-C8-C9	107.4(3)
C7-C8-H8	126.3	C9-C8-H8	126.3
C16-C9-N2	126.0(3)	C16-C9-C8	123.5(3)
N2-C9-C8	110.5(3)	C15-C10-C11	117.8(3)
C15-C10-C5	122.0(3)	C11-C10-C5	120.2(3)
C12-C11-C10	121.0(3)	C12-C11-H11	119.5
C10-C11-H11	119.5	C11-C12-C13	119.8(3)
C11-C12-H12	120.1	C13-C12-H12	120.1
C14-C13-C12	120.1(3)	C14-C13-S1	119.9(2)
C12-C13-S1	120.0(2)	C15-C14-C13	119.8(3)
C15-C14-H14	120.1	C13-C14-H14	120.1
C14-C15-C10	121.4(3)	C14-C15-H15	119.3
C10-C15-H15	119.3	C9-C16-C1	122.0(3)
C9-C16-C17	119.5(3)	C1-C16-C17	118.5(3)
C22-C17-C18	117.5(3)	C22-C17-C16	120.7(3)

C18-C17-C16	121.8(3)	C19-C18-C17	121.6(3)
C19-C18-H18	119.2	C17-C18-H18	119.2
C18-C19-C20	119.0(3)	C18-C19-H19	120.5
C20-C19-H19	120.5	C21-C20-C19	120.6(3)
C21-C20-S2	119.7(3)	C19-C20-S2	119.6(3)
C20-C21-C22	119.7(3)	C20-C21-H21	120.2
C22-C21-H21	120.2	C21-C22-C17	121.5(3)
C21-C22-H22	119.3	C17-C22-H22	119.3
C26-N3-C23	107.4(2)	C26-N3-H3A	126.3
C23-N3-H3A	126.3	C31-N4-C28	107.6(2)
C31-N4-H4	126.2	C28-N4-H4	126.2
C34-N5-C35	119.9(3)	C34-N5-C37	120.2(3)
C35-N5-C37	119.9(3)	C41-N6-C40	120.5(3)
C41-N6-C43	119.0(3)	C40-N6-C43	120.4(3)
C31-C00Z-C23	127.0(3)	C31-C00Z-C38	117.5(3)
C23-C00Z-C38	115.4(3)	N3-C23-C00Z	126.0(3)
N3-C23-C24	108.9(3)	C00Z-C23-C24	125.1(3)
C25-C24-C23	107.4(3)	C25-C24-H24	126.3
C23-C24-H24	126.3	C24-C25-C26	107.3(3)
C24-C25-H25	126.3	C26-C25-H25	126.3
N3-C26-C27	125.6(3)	N3-C26-C25	109.0(3)
C27-C26-C25	125.4(3)	C28-C27-C26	124.6(3)
C28-C27-C32	118.9(3)	C26-C27-C32	116.5(3)
N4-C28-C27	125.0(3)	N4-C28-C29	108.7(3)
C27-C28-C29	126.3(3)	C30-C29-C28	107.5(3)
C30-C29-H29	126.2	C28-C29-H29	126.2
C29-C30-C31	107.7(3)	C29-C30-H30	126.1
C31-C30-H30	126.1	N4-C31-C00Z	126.2(3)
N4-C31-C30	108.4(3)	C00Z-C31-C30	125.3(3)
C36-C32-C33	116.3(3)	C36-C32-C27	123.0(3)
C33-C32-C27	120.6(3)	C34-C33-C32	120.7(3)
C34-C33-H33	119.6	C32-C33-H33	119.6
N5-C34-C33	121.2(3)	N5-C34-H34	119.4
C33-C34-H34	119.4	N5-C35-C36	121.3(3)
N5-C35-H35	119.4	C36-C35-H35	119.4
C35-C36-C32	120.6(3)	C35-C36-H36	119.7
C32-C36-H36	119.7	N5-C37-H37A	109.5
N5-C37-H37B	109.5	H37A-C37-H37B	109.5
N5-C37-H37C	109.5	H37A-C37-H37C	109.5
H37B-C37-H37C	109.5	C39-C38-C42	116.9(3)
C39-C38-C00Z	122.8(3)	C42-C38-C00Z	120.3(3)
C40-C39-C38	120.0(3)	C40-C39-H39	120.0

C38-C39-H39	120.0	N6-C40-C39	121.3(3)
N6-C40-H40	119.4	C39-C40-H40	119.4
N6-C41-C42	120.5(3)	N6-C41-H41	119.8
C42-C41-H41	119.8	C41-C42-C38	120.8(3)
C41-C42-H42	119.6	C38-C42-H42	119.6
N6-C43-H43A	109.5	N6-C43-H43B	109.5
H43A-C43-H43B	109.5	N6-C43-H43C	109.5
H43A-C43-H43C	109.5	H43B-C43-H43C	109.5
H7A-O7-H7B	104.44(15)	H7C-O7A-H7D	104.44(15)
H8A-O8-H8B	104.42(15)	H9A-O9-H9B	104.43(15)
H10A-O10-H10B	104.43(15)	H11A-O11-H11B	104.41(15)

Table S6. Anisotropic atomic displacement parameters (Å^2) for H_2TMPyP:NiTSPP crystal structure						
	U_{11}	U_{22}	U_{33}	U_{23}	U_{13}	U_{12}
Ni1	0.0267(4)	0.0133(3)	0.0157(3)	0.0005(2)	0.0035(2)	-0.0007(2)
S1	0.0451(6)	0.0153(4)	0.0396(5)	0.0019(3)	0.0143(4)	0.0030(3)
S2	0.0418(6)	0.0549(6)	0.0233(4)	0.0084(4)	0.0081(4)	0.0055(4)
O1	0.069(2)	0.0237(12)	0.0441(15)	-0.0019(11)	0.0224(13)	0.0069(12)
O2	0.0437(16)	0.0212(12)	0.0599(17)	0.0006(11)	0.0095(12)	-0.0009(10)
O3	0.0421(15)	0.0220(12)	0.0560(16)	0.0038(11)	0.0132(12)	0.0069(10)
O4	0.0328(15)	0.071(2)	0.0291(14)	0.0148(13)	0.0050(11)	0.0005(13)
O5	0.0432(17)	0.0666(19)	0.0357(15)	0.0222(13)	0.0076(12)	0.0150(14)
O6	0.071(2)	0.068(2)	0.0264(14)	-0.0066(13)	0.0096(14)	-0.0051(16)
O4A	0.055(11)	0.089(18)	0.05(3)	-0.009(18)	0.005(12)	0.019(11)
O5A	0.061(9)	0.034(17)	0.04(2)	0.003(15)	-0.005(12)	0.018(9)
O6A	0.10(2)	0.069(8)	0.05(3)	-0.004(9)	0.007(19)	-0.007(8)
N1	0.0262(15)	0.0172(12)	0.0210(12)	0.0013(10)	0.0049(10)	-0.0009(10)
N2	0.0262(15)	0.0157(12)	0.0189(12)	-0.0010(9)	0.0029(10)	-0.0020(10)
C1	0.0273(17)	0.0200(14)	0.0165(14)	0.0012(11)	0.0042(12)	-0.0008(12)
C2	0.0296(19)	0.0242(16)	0.0215(15)	0.0011(12)	0.0070(13)	0.0016(13)
C3	0.0315(19)	0.0218(15)	0.0243(15)	-0.0009(12)	0.0057(13)	0.0028(13)
C4	0.0268(17)	0.0174(14)	0.0211(14)	-0.0009(11)	0.0031(12)	0.0007(12)
C5	0.0261(17)	0.0171(14)	0.0227(15)	-0.0009(12)	0.0013(12)	0.0006(12)
C6	0.0280(17)	0.0164(14)	0.0212(14)	-0.0004(11)	0.0016(12)	-0.0025(12)
C7	0.0323(19)	0.0169(14)	0.0244(16)	0.0020(12)	0.0009(13)	0.0004(13)
C8	0.0336(19)	0.0204(15)	0.0192(14)	0.0033(12)	0.0014(13)	-0.0015(13)
C9	0.0257(17)	0.0179(14)	0.0195(14)	0.0026(11)	0.0004(12)	-0.0028(12)
C10	0.0277(18)	0.0166(14)	0.0233(15)	0.0011(12)	0.0077(13)	-0.0006(12)
C11	0.0267(18)	0.0202(14)	0.0219(15)	0.0027(12)	0.0072(13)	0.0024(12)
C12	0.0326(19)	0.0212(15)	0.0217(15)	0.0000(12)	0.0104(13)	-0.0021(13)
C13	0.0305(19)	0.0151(14)	0.0330(17)	0.0029(12)	0.0144(14)	0.0004(13)
C14	0.0302(19)	0.0212(15)	0.0320(17)	0.0067(13)	0.0071(14)	0.0031(13)
C15	0.0295(19)	0.0225(15)	0.0263(16)	0.0028(12)	0.0051(13)	-0.0005(13)
C16	0.0268(18)	0.0180(14)	0.0199(14)	-0.0002(11)	0.0013(12)	-0.0016(12)
C17	0.0289(18)	0.0207(15)	0.0204(15)	0.0046(12)	0.0062(13)	0.0052(13)
C18	0.0323(19)	0.0253(16)	0.0242(16)	0.0024(12)	0.0032(13)	-0.0005(13)
C19	0.036(2)	0.0303(17)	0.0271(17)	0.0092(14)	0.0096(14)	0.0040(15)
C20	0.033(2)	0.0369(19)	0.0226(16)	0.0045(14)	0.0080(14)	0.0125(15)
C21	0.0317(19)	0.0349(18)	0.0236(16)	-0.0035(14)	0.0026(14)	0.0088(15)
C22	0.0307(19)	0.0249(16)	0.0235(15)	-0.0001(12)	0.0033(13)	0.0032(13)
N3	0.0308(15)	0.0177(12)	0.0213(12)	0.0013(10)	0.0054(11)	-0.0001(11)
N4	0.0314(16)	0.0175(12)	0.0200(12)	0.0016(10)	0.0050(11)	-0.0012(11)

N5	0.0311(16)	0.0320(15)	0.0214(13)	-0.0025(11)	0.0049(11)	-0.0070(12)
N6	0.0346(17)	0.0161(12)	0.0333(15)	0.0040(11)	0.0154(12)	0.0007(11)
C00Z	0.0289(18)	0.0178(14)	0.0231(15)	0.0018(12)	0.0033(13)	-0.0012(12)
C23	0.0301(18)	0.0171(14)	0.0224(14)	0.0017(12)	0.0058(13)	0.0019(12)
C24	0.036(2)	0.0199(15)	0.0259(16)	0.0033(12)	0.0077(14)	-0.0027(13)
C25	0.037(2)	0.0205(15)	0.0232(15)	0.0000(12)	0.0132(14)	-0.0025(14)
C26	0.0309(18)	0.0188(14)	0.0206(15)	0.0022(11)	0.0056(13)	0.0004(13)
C27	0.0267(18)	0.0214(15)	0.0208(14)	0.0004(12)	0.0045(12)	-0.0005(12)
C28	0.0300(18)	0.0181(14)	0.0196(14)	0.0011(11)	0.0030(13)	0.0003(12)
C29	0.0327(19)	0.0196(15)	0.0195(14)	-0.0017(11)	0.0031(13)	0.0007(13)
C30	0.0314(18)	0.0156(14)	0.0227(15)	0.0017(11)	0.0034(13)	-0.0021(12)
C31	0.0280(17)	0.0162(14)	0.0211(14)	0.0005(11)	0.0046(12)	0.0002(12)
C32	0.0259(18)	0.0185(14)	0.0211(15)	0.0016(11)	0.0063(12)	-0.0046(12)
C33	0.034(2)	0.0252(16)	0.0259(16)	0.0014(13)	0.0052(14)	0.0020(14)
C34	0.035(2)	0.0336(18)	0.0222(15)	0.0028(13)	0.0035(14)	0.0000(15)
C35	0.0291(19)	0.0246(16)	0.0279(16)	-0.0040(13)	0.0043(14)	-0.0038(13)
C36	0.0296(18)	0.0204(15)	0.0213(14)	-0.0002(12)	0.0038(13)	-0.0028(13)
C37	0.038(2)	0.050(2)	0.0205(16)	-0.0026(15)	0.0076(14)	-0.0044(17)
C38	0.0286(18)	0.0169(15)	0.0230(15)	-0.0001(12)	0.0103(13)	0.0023(12)
C39	0.0266(18)	0.0212(15)	0.0267(16)	-0.0013(12)	0.0085(13)	0.0023(13)
C40	0.0293(19)	0.0217(16)	0.0333(17)	-0.0032(13)	0.0117(14)	0.0005(13)
C41	0.035(2)	0.0234(16)	0.0262(16)	0.0048(13)	0.0102(14)	0.0043(14)
C42	0.0333(19)	0.0213(15)	0.0258(16)	0.0020(12)	0.0082(14)	-0.0008(13)
C43	0.044(2)	0.0193(16)	0.048(2)	0.0097(14)	0.0160(17)	-0.0003(15)
O7	0.149(19)	0.064(13)	0.111(17)	0.022(13)	-0.009(15)	-0.022(13)
O7A	0.087(7)	0.114(8)	0.118(8)	0.049(7)	-0.022(6)	-0.017(6)
O8	0.078(3)	0.055(2)	0.0423(19)	0.0045(16)	0.0180(17)	0.015(2)
O9	0.073(2)	0.0444(16)	0.0600(19)	0.0009(14)	0.0008(16)	0.0076(15)
O10	0.081(2)	0.0485(17)	0.0595(19)	-0.0143(15)	0.0178(18)	0.0105(16)
O11	0.112(3)	0.0522(19)	0.060(2)	0.0091(16)	-0.0017(19)	0.016(2)

References

1 M. Adinehnia, B. Borders, M. Ruf, B. Chilukuri, K.W.Hipps and U. Mazur, *J. Mat. Chem. C.,* 2016, **5**, 10223-10239.

2 D. H. Karweik and N. Winograd, *Inorg. Chem.,* 1976**, 15**, 2336-2342.

3 J. P. Macquet, M. M. Millard and T. Theophanides, *J. Am. Chem. Soc.,* 1978, **100**, 4741-4746.

4 R. J. J. Jansen and H. Vanbekkum, *Carbon,* 1995**, 33**, 1021-1027.

5 L. Silipigni, G. De Luca, Q. Quattrone, L. M. Scolaro, G. Salvato and V. J. Grasso, *Phys.: Condens. Matter.,* 2006**, 18**, 5759-5772.

6 H. Marbach, *Acc. Chem. Res.* 2015, **48**, 2649–2658.

7 I. Reid, Y. Zhang, A. Demasi, A. Blueser, L. Piper, J. E. Downes, A. Matsuura, G. Hughes and K. E. Smith, *Appl. Surf. Sci.* 2009, **256**, 720–725.

8 G. M. Sheldrick, *SHELXS-2014, Program for Crystal Structure Solution*, University of Göttingen, 2014.

9 G. M. Sheldrick, SHELXS-2014, Program for Crystal Structure Solution, University of Gottingen, 2014.